WYLE LABORATORIES - RESEARCH STAFF

REPORT WR 67-12

THE VISUALIZATION OF TURBULENT FLOWS BY MEANS OF FLOW BIREFRINGENCE

by

Eric B. Miller

Submitted as a Summary Report Under Contract NAS8-5384, Task 15

Prepared by Eric B. Miller
Eric B. Miller

Approved by R.C. Kao for R.C.P.
R.C. Potter
Program Manager

Approved by
L.C. Sutherland
Director of Research Staff, Huntsville

Date July 1967

COPY NO. 6

SUMMARY

Flow birefringence is discussed as a technique for the qualitative investigation of separated flows. The results of high speed motion picture studies of unsteady flows through various geometries are discussed. Photographs of many of the observed phenomena are also presented. Recommendations are made for the design of an optimum flow system. It is concluded that the technique is of great value qualitatively and holds promise for development into a quantitative method for studying unsteady flows. An approach is suggested whereby the birefringent visualization of two dimensional flows could be extended more readily to three dimensional flows. Further study into the relationships between large eddies in turbulent shear regions and the associated mean flow properties is recommended.

TABLE OF CONTENTS

TABLE OF CONTENTS (Continued)

LIST OF FIGURES

LIST OF SYMBOLS

A	a constant defined in Equation A7
AA'	a line specifying the transmission axis of an analyzer
$A_{1,2}$	the amplitude of the optical vector along axes 1 or 2 in a birefringent medium
B	a constant defined in Equation A7
c	the propagation velocity for light in a vacuum
d	the optical path length in a birefringent medium
D	the diameter of a jet orifice (Figure 14)
$\vec{E}$	the optical vector for a monochromatic light ray
E_o	the total energy of the outer vortex ring lamina (a constant)
E_{ROT}	the rotational energy of the outer vortex ring lamina
E_{TRANS}	the translational energy of the outer vortex ring lamina in R direction
G	velocity gradient (shear rate)
I	the moment of inertia of the outer vortex ring lamina
k	a constant defined in Equation A4
K	an index used in specifying ϕ
L	angular momentun of the outer vortex ring lamina
M	the mass of the outer vortex ring lamina
n	index of refraction; $(n = c/v)$ if v is the propagation velocity of light in a medium
PP'	a line specifying the transmission axis of a polarizer
R	the radius of a vortex ring section (Figure 13)

LIST OF SYMBOLS (Continued)

R_o	the radius of a vortex ring at an arbitrary zero position along the jet axis (Figure 13)
t	time
T	the period of vibration of the optical vector
$\vec{u}, \vec{v}$	unit vectors specifying an optical axis in a birefringent medium
v	the axial velocity in a circular, constant density free jet
v_p	the velocity in the laminar core of the jet
v_r	a velocity defined in Equation A11 of Appendix A
x	coordinate of length along the jet axis
x_c	the location of the center of mass of a vortex ring along the jet axis (Figure 13)
y	the transverse coordinate perpendicular to the jet axis (Figure 13)

Greek Symbols

α	an angle defining the spread of a constant density jet
α_1, α_2	constants in a form of the Powell-Eyring equation for pseudo-plastics
δ	the thickness of the outer vortex ring lamina (a constant)
λ_o	the wavelength of a monochromatic light ray in a vacuum ($\lambda_o = cT$)
μ	viscosity
μ_o	viscosity at zero velocity gradient
μ_∞	limiting value of viscosity at very high velocity gradients
ρ	density
ϕ	the phase difference between the two components of the optical vector, $\vec{E}$, upon traveling through a birefringent medium

LIST OF SYMBOLS (Continued)

Ψ	the angle between the plane of polarization of the optical vector and an axis in a birefringent medium
ω	angular velocity
ω_o	the angular velocity of the vortex ring lamina at an arbitrary zero position along the jet axis

1.0 INTRODUCTION

The phenomenon of flow double refraction or "streaming birefringence" was known to exist at least as early as 1873 when J.C. Maxwell (Reference 1) submitted a paper to the Royal Society of London, describing the effect which he observed when stirring a sample of Oregon balsam between Nicol prisms.

Since Maxwell's paper, much work has been done using bentonite ($Al_2O_3 \cdot 4SO_2 \cdot H_2O$) or colloidal solutions of vanadium pentoxide to simulate and visualize flows of other fluids. Flow birefringence has been used extensively in the design of aerodynamic or hydrodynamic bodies. An example of this is the investigation of flows around automobile bodies by Hauser and Dewey (Reference 2). Biological applications of this phenomenon include the simulation of blood flows through prosthetic, circulatory-assist devices (References 3, 4, 5, and 6) and its recent use in the study of naturally occurring flows in a microorganism (Reference 7). These applications of flow birefringence produced results which were qualitative but which provided valuable insights into the nature of flow fields that are bounded by complex geometries.

Peebles, et al., relying somewhat on the earlier theoretical contributions of Rosenberg (Reference 8) have taken a step toward placing birefringent flow visualization on a firmer quantitative base, using a commercial dyestuff known as milling yellow dye suspension (MYDS). They have used aqueous suspensions of MYD to verify the applicability of the Navier-Stokes equations to two-dimensional laminar flows (References 9, 10, 11, and 12) and have studied the rheological properties of MYDS extensively (References 13, 14). This work has established that aqueous MYDS is a member of a class of fluids known as "pseudo-plastics" which are non-Newtonian in character. Further, it has been shown that aqueous suspensions of MYD obey the Powell-Eyring relation between viscosity and velocity gradient (Reference 14).

Despite the success in quantitative work with well-behaved laminar flows, a theoretical treatment which makes MYDS useful in quantitative studies of turbulence or transition flows has not yet been advanced.

The photographs which appear in this report were obtained using the visualization technique of flow double refraction, with MYDS as the visulaization fluid. This approach can be criticized if observations on the flow of non-Newtonian MYDS are extrapolated to Newtonian fluids. However, it is doubtful that the gross features (large eddy structure, turbulence, changes in turbulent scale, etc.) in the flow of the two types of fluid are significantly different. Also, this approach makes location of probes in the flow unnecessary and thereby eliminates a serious experimental restriction. The qualitative insights obtained with this technique justify its use in spite of the fact that exact scaling of the observed flow phenomena to flows of Newtonian fluids is not possible.

This report will apply the flow visualization technique of flow birefringence to unsteady flow phenomena associated with "separated flows." The separation phenomena, which are studied, arise as a result of flow in either direction over a vertical discontinuity in the width of a horizontal two-dimensional flow channel. Jet flow and channel flow will also be considered, since these may be regarded as the special cases of infinite discontinuity and zero discontinuity, respectively.

Emphasis will be placed on observations of the large scale eddy structure, and an effort will be made to infer the mean flow properties from these observations. The difference between large scale eddy structure in MYDS and in similar flows of Newtonian fluids is considered to be minor.

2.0 THEORETICAL CONSIDERATIONS - MONOCHROMATIC LIGHTING

2.1 Double Refraction of Monochromatic Light

A double refracting or "birefringent" material is one which exhibits different propagation velocities for optical vibrations in different internal planes or "axes", which are parallel to the direction of propagation. Vibrations of the optical vector are, of course, perpendicular to the direction of propagation. A material having birefringent properties is considered to have two indices of refraction, n_1 and n_2, since the index of refraction, n, is commonly defined by the equation,

$$n = \frac{c}{v} , \qquad (1)$$

where v is the propagation velocity for light in the medium and c is the velocity of light in a vacuum.

Figure 1 illustrates a wave of plane-polarized, monochromatic light which is incident upon a birefringent medium. The propagation direction is perpendicular to the page.

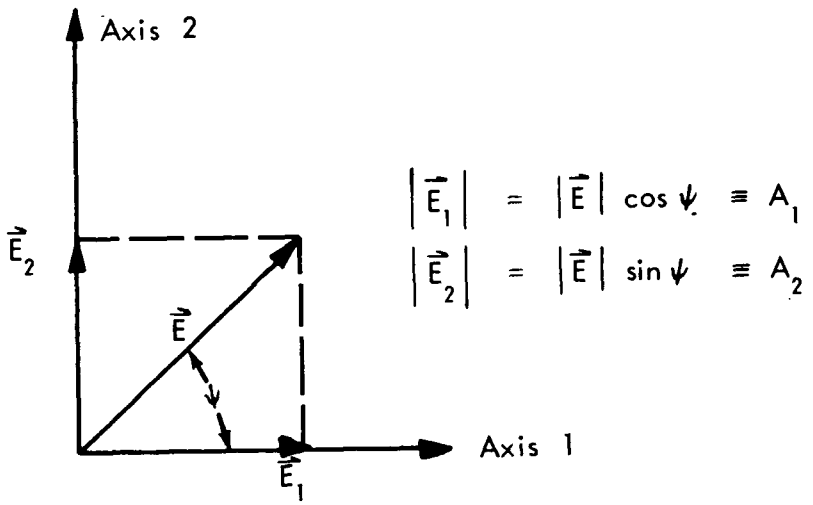

Figure 1. This sketch shows the orientation of the incident, plane-polarized, optical vector $\vec{E}$ with respect to Axis 1 and Axis 2 of the birefringent medium.

The amplitudes of the components of the optical vector along Axis 1 and Axis 2 are A_1 and A_2 respectively.

Resolving the incident optical vector along the two axes in the medium permits one to determine the phase change between $\vec{E}_1$ and $\vec{E}_2$ that results from motion through the medium. To accomplish this, it is only necessary to use different propagation velocities along Axis 1 and Axis 2, which, by Equation 1, may be given by c/n_1 and c/n_2, respectively.

Before entering the material,

$$E_1 = A_1 \cos 2\pi \frac{t}{T}, \quad \text{and}$$
$$E_2 = A_2 \cos 2\pi \frac{t}{T} \quad . \tag{2}$$

After leaving the material,

$$E_1 = A_1 \cos \frac{2\pi}{T}\left[t - \frac{n_1 d}{c}\right] = A_1 \cos 2\pi\left[\frac{t}{T} - \frac{n_1 d}{\lambda_o}\right],$$

and (3)

$$E_2 = A_2 \cos \frac{2\pi}{T}\left[t - \frac{n_2 d}{c}\right] = A_2 \cos 2\pi\left[\frac{t}{T} - \frac{n_2 d}{\lambda_o}\right]$$

where d is the thickness of the material and λ_o $(= cT)$ is the wavelength of the monochromatic light in a vacuum. Thus, the oscillation parallel to Axis 1 lags that parallel to Axis 2 by the phase angle,

$$\phi = \frac{2\pi d}{\lambda_o}(n_1 - n_2) \tag{4}$$

It is possible to change the reference time for the emerging beam so that,

$$E_1 = A_1 \cos \frac{2\pi t}{T}$$

and (5)

$$E_2 = A_1 \cos\left(\frac{2\pi t}{T} + \phi\right)$$

Eliminating the time, t , between these two equations (Equations 5) produces an equation which represents the projection on the (1, 2) plane of the trajectory of a hypothetical particle having a position vector equal to the optical vector, $\vec{E}$. The resulting equation is that of an ellipse.

$$\frac{E_1^2}{A_1^2} + \frac{E_2^2}{A_2^2} - \frac{2E_1 E_2 \cos\phi}{A_1 A_2} = \sin^2\phi \qquad (6)$$

The polarization of the emerging beam is defined by Equation 6. In general, a plane polarized, monochromatic beam will become elliptically polarized upon traveling through a birefringent medium. Obvious simplifications in Equation 6 result if ϕ is allowed to take on certain values.

Condition 1: $\phi = 2\pi K$, $K = 1, 2, 3, \ldots$. etc. The emerging beam will be plane-polarized with vibrations in the same plane as the incident beam.

Condition 2: $\phi = (2K + 1)\,\pi$, $K = 1, 2, 3, \ldots$. etc. The emerging beam will be plane-polarized in a direction making an angle of 2ψ with the incident beam.

Condition 3: $\phi = (K + \frac{1}{2})\pi$, $\psi = \frac{\pi}{4}$, $K = 1, 2, 3, \ldots$. etc. The emerging beam will be circularly polarized in this case.

These conditions may be verified by substitution into Equation 6.

3.0 THEORETICAL CONSIDERATIONS - WHITE LIGHTING

3.1 The Effect of a Doubly Refracting Medium on White Light

In order to simplify this discussion, the results of the previous section will be used and the system which is illustrated in Figure 2 will be considered. In this figure, the transmission axes of the analyzer and polarizer are at 90^{o} to one another and at 45^{o} to the axes of the birefringent medium, $\vec{u}$ and $\vec{v}$.

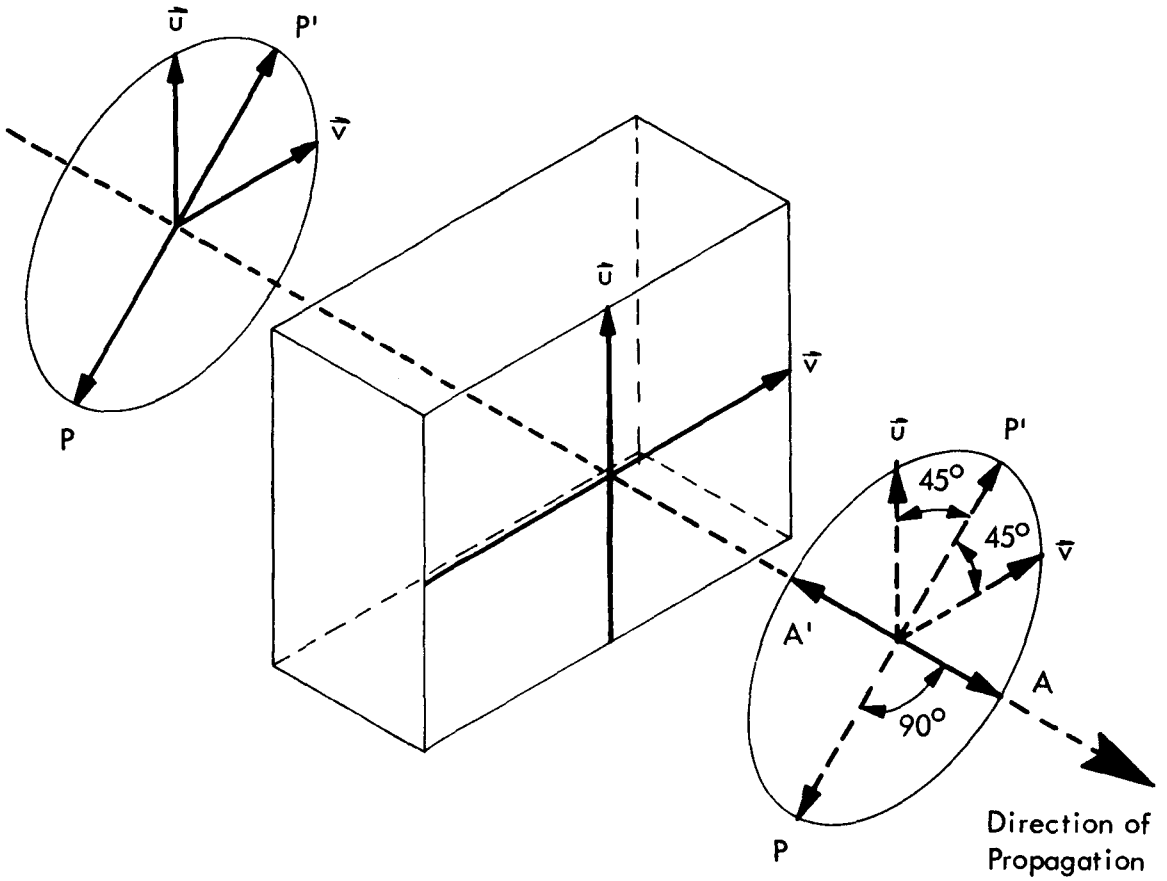

Figure 2. A sample of birefringent material is shown between two ideal linear polarizers. $\vec{u}$ and $\vec{v}$ are unit vectors defining the optical axes of the birefringent medium. PP' defines the transmission axes of the polarizer while AA' defines the transmission axis of the analyzer.

From Condition 1 in the previous section, it is apparent that all wavelengths which satisfy the condition,

$$K\lambda_o = d(n_u - n_v) \tag{7}$$

leave the birefringent medium linearly polarized in a plane parallel to axis PP'. Rays with these wavelengths are completely stopped by the analyzer since AA' is perpendicular to PP'.

Rays with wavelengths which satisfy the condition,

$$(2K + 1)\frac{\lambda_o}{2} = d(n_u - n_v) \tag{8}$$

emerge from the birefringent medium with their plane of vibration parallel to transmission axis AA' (Condition 2 in the previous section). These rays are transmitted without attenuation by the analyzer.

Rays having wavelengths that lie between those wavelengths which satisfy conditions (7) and (8), willemerge from the birefringent medium with elliptical or circular polarization and be partially transmitted by the analyzer.

Color in the image seen through the analyzer is thus a result of the fact that some wavelengths are missing while others are totally transmitted.

If AA' is oriented so that it is parallel to PP' while both AA' and PP' are still 45° from the two axes in the birefringent medium, Equation 8 becomes the condition of lowest intensity while Equation 7 becomes the condition of maximum intensity. With this configuration, the transmitted colors will be such that they produce white when added to the colors obtained with AA' perpendicular to PP'. Colors which sum to produce white are said to be "complementary".

3.2 The Effect of Optical Path Length on Color in a Birefringent Medium

Rossi (Reference 15) has shown, very simply, that an increase in thickness of the birefringent medium reduces the coloring of the image as seen through the analyzer.

This fact is demonstrated by considering two neighboring wavelengths, each

corresponding to an intensity maximum. These wavelengths satisfy the equations,

$$K\lambda_1 = d(n_u - n_v) \tag{9}$$

and

$$(K + 1)\lambda_2 = d(n_u - n_v) \tag{10}$$

From Equations 9 and 10 can be obtained the relationships,

$$\frac{\lambda_1}{\lambda_2} = 1 + \frac{1}{K} = 1 + \frac{\lambda_1}{d(n_u - n_v)} \tag{11}$$

This equation shows that λ_1/λ_2 approaches unity as d increases. It thus becomes more difficult to distinguish colors as the thickness of the birefringent medium increases. For this reason a compromise must often be made in flow studies using birefringent fluids. This compromise is between the depth of fluid, d, which assures valid two dimensional flows, and brightness of color, which provides better definition or detail of the flow field.

4.0 THE INVESTIGATION OF LAMINAR TWO-DIMENSIONAL FLOW FIELDS USING FLOW BIREFRINGENCE

Although the primary purpose of this report is the presentation of the results of a qualitative study of unsteady flow phenonena in separated flow, some mention should be made of the extent to which flow birefringence has been developed as a tool for obtaining quantitative information. In order to do this, at least a cursory knowledge of the terms and experimental methods is required.

When a birefringent fluid is caused to flow in a laminar manner between polarizers and is viewed by light traversing both the polarizers and the fluid, interference patterns are observed. Generally, with laminar flow, these patterns are composed of alternating colored and dark bands. The bands are stationary in steady laminar flow but become random and rapidly varying in turbulent flow. One type of band is called an isochromatic and, may be used to determine the maximum velocity gradient in the fluid. The other is called an isoclinic and is related to the direction of the maximum velocity gradient.

It is generally agreed that birefringence in suspensions is due to the orientation of particles, which are other than spherical in shape, with respect to the flow streamlines. This orientation is considered to be a result of the action of hydrodynamic forces on the particles. In the case of pure liquids, however, the effect is thought to be due to molecular deformation rather than orientation. Double refraction cannot be readily observed in the case of pure liquids and special equipment is required in this case. However, the flow analysis is easier in the case of pure liquids because of the closer analogy between the hydrodynamic and photoelastic cases. Wayland (Reference 16) has studied solutions of pure ethyl cinnamate, which has a low optical sensitivity, using a compensator to determine the amount of double refraction. Such studies must be conducted on a point by point basis.

The isoclinic may be defined in a more satisfying manner if the orientation of particles in the flow is taken as a valid explanation of the flow birefringence phenomenon. An isoclinic may then be defined as the location of all particles whose optic axes make a fixed angle with some arbitrarily chosen reference line. Alternately, an isoclinic can be defined as the location of all particles with optic axes which are aligned with the transmission axes of either the linear polarizer or linear analyzer. These transmission axes must be at 90° to one another and bear a constant relationship to axes in the birefringent medium. No light passes completely through the system in this case, so that all isoclines appear as dark lines. The dark lines disappear if the medium is illuminated with circularly rather than linearly-polarized monochromatic light. For this reason the isoclines are frequently determined by comparing the images produced by illuminating the medium with linear and then circularly-polarized monochromatic light. Circularly-polarized light may be produced very simply by inserting a quarter wave plate

between a linearly-polarized monochromatic light source and the birefringent medium. Another method is to reverse a commercially available composite, which is a quarter wave plate bonded to a linear polarizer. Monochromatic light traversing the composite in one direction is linearly polarized and in the other direction is circularly polarized.

If the streamline direction is known at a point in the flow, an angle may be experimentally determined which specifies the orientation of the optic axis of a particle with respect to the streamline, at this same point. This is accomplished by choosing the arbitrary reference line mentioned above to coincide with the streamline direction. The crossed linear polarizer and linear analyzer may then be rotated as a unit from the streamline direction until extinction occurs. The angle swept out in this operation is known as the extinction angle.

The birefringence of a fluid may be put on a quantitative basis by use of an equation of the type,

$$N = \frac{\mu t G}{n} \tag{12}$$

where μ is the viscosity, t is the optical path, n is the number of observed fringes and G is the velocity gradient. N is determined experimentally in a concentric cylinder device. It is considered a measure of the birefringence and is called the fringe value.

If the fluid is located in the annular region between two concentric cylinders, one of which is rotating, the streamline direction is simply a perpendicular to the radius of the cylinders at the point of interest. Such a device is commonly used to calibrate birefringent fluids since it makes possible quantitative determinations of the extinction angle and the amount of birefringence. It may also be used as a Couette viscometer to measure the viscosity of the fluid.

Because of the temperature and concentration sensitivities of birefringent suspensions, all of these measurements must be performed under carefully controlled conditions. Evaporation must be kept to a minimum and temperature carefully regulated.

Most birefringent suspensions are temperature sensitive. The amount of birefringence decreases with increasing temperature. A possible explanation for this effect is the action of Brownian motion on the suspended particles. Since the intensity of Brownian motion increases with temperature the two observed effects show the proper trends. Boeder (Reference 17) has investigated the effect of Brownian motion from a theoretical standpoint and concluded that both the angle between

the particle axis and the streamline, and the birefringence were functions of the intensity of Brownian motion.

5.0 VARIOUS CHARACTERISTICS OF MILLING YELLOW DYE SUSPENSIONS

It has been observed experimentally (Reference 10), that isoclinic patterns obtained using Milling Yellow Suspensions are poorly defined. It was therefore useful to develop methods of quantitative flow analysis based upon the isochromatic lines (References 11 and 12).

MYDS is known to obey the Powell-Eyring relation between velocity gradient and viscosity which applies to "pseudo-plastics"(Reference 14). The viscosity, μ, is related to the velocity gradient, G, by the equation,

$$\mu = \mu_\infty + \frac{A(\mu_o - \mu_\infty) \sinh^{-1}\left(\frac{G}{A}\right)}{G} \quad , \tag{13}$$

where μ_∞ , μ_o and A are constants. For low velocity gradients,

$$\sin^{-1}\left(\frac{G}{A}\right) \cong \frac{G}{A} \quad , \tag{14}$$

so that

$$\mu = \mu_o \cdot \tag{15}$$

For high velocity gradients,

$$\sinh^{-1}\left(\frac{G}{A}\right) \cong \ell n\left(\frac{2}{A}\right) + \ell n\, G, \tag{16}$$

so that

$$\mu = \mu_\infty + \frac{\alpha_1}{G} + \alpha_2 \frac{\ell n\, G}{G} \quad . \tag{17}$$

where α_1 and α_2 are constants. In Equation 17, μ approaches μ_∞

asymptotically as the velocity gradient becomes large. Figure 3 shows these trends in a plot of μ versus G, for a solution of MYDS. Since $\mu = \mu_o$, and the number of observed fringes is linearly related to the velocity gradient for low velocity gradients, MYDS is useful for analysis of low-speed, laminar, Newtonian flows. The accuracy of such analyses is on the order of $\pm$ 10 percent for flow in straight streamliners and within $\pm$ 15 percent for flow in straight non-parallel streamlines (Reference 10). The analysis is not straight-forward and must be conducted numerically. This technique is limited to two dimensional flows having essentially constant flow patterns. Analysis may be conducted using either isoclinics and isochromatics (Reference 10), or isochromatics alone (References 11 and 12).

MYDS will probably never become generally useful for quantitative analysis of turbulent Newtonian flows because of its non-Newtonian properties. It seems possible that a point by point, statistical analysis of turbulent flow fields using an advanced optical system and the birefringence of pure liquids holds some promise. Pure liquids are more Newtonian in character and the method for relating photoelastic theory and hydrodynamics appears simpler when they are considered.

When white light is used with MYDS as the birefringent medium, the following colors are observed, providing the transmission axes of the polarizer and analyzer are at 90° to one another.

Color	Fringe Order
Black	0
Yellow	1
Red	2
Green	3
Yellow	4
Red	5
Green	6
Yellow	7
.	.
.	.
etc.	etc.

If the transmission axes of the polarizer and analyzer are parallel, the zero order is white and the complementary colors are observed. The absence of the blue spectral region is a result of the fact that MYDS absorbs these wavelengths readily. This point has been noted by Thurston (Reference 18).

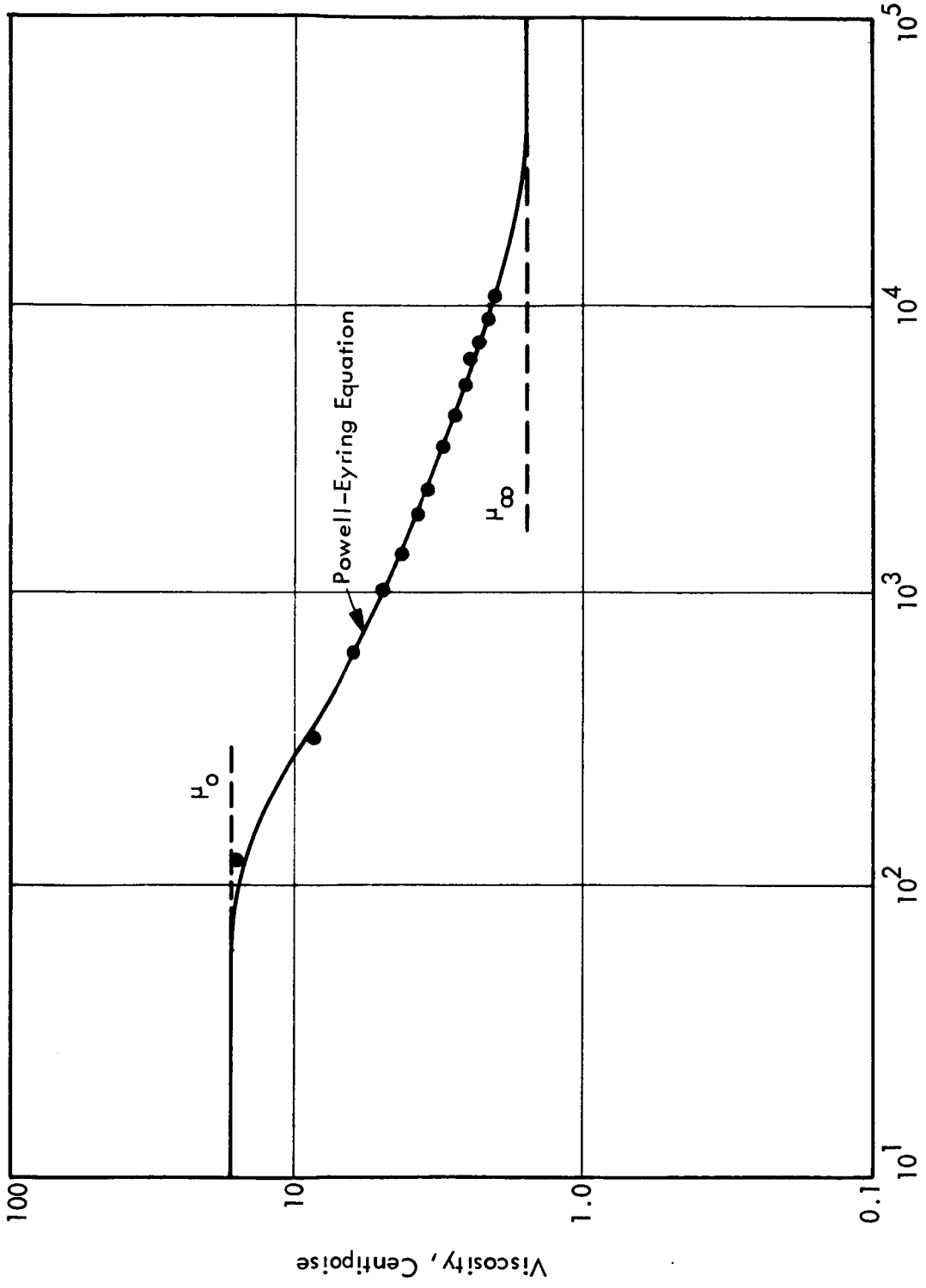

Figure 3. Viscosity Data for 1.32% Aqueous Milling Yellow Suspension at 25° C.

MYDS, unlike bentonite sols, is not thixotropic. That is, the viscosity and sensitivity of MYDS are not related to the amount of mechanical work done on it. However, the presence of certain materials, notably copper, brass, and possibly lead, have been observed to cause changes in the properties of MYDS. Because of this, it is better to build a flow system chiefly from stainless steel, plastics and glass, which cause no changes in the physical properties of the suspension.

6.0 APPARATUS

6.1 Design of Flow System

The system pictured in Figure 4 and shown schematically in Figure 5 was designed for flexibility. It can be operated using a constant-head gravity feed from reservoir 6 (Figure 5) with the pump used to maintain the head. Also, pneumatic pressurization of reservoir 6 using pressure regulators will provide flow through the visualization section. The complete schematics for these cases are not shown in Figure 5. Direct coupling of the pump to the visualization section is also possible.

Velocities, which were high enough to observe unsteady flow, were not possible using a gravity feed system, without considerable inconvenience, and a pneumatic pressure line was not available within the time alotted for the project. Therefore, it was necessary to use a centrifugal pump to provide the flow.

The sensitivity of MYDS to certain metals made necessary the construction of this system from plastics and stainless steel. Polyethylene, "Nylon", acrylic plastic, and stainless steel were therefore used in construction and no interaction between the fluid and this system has been observed.

The use of a turbine flow meter and a centrifugal pump in the flow system is questionable. It was determined by stroboscopic examination of the flow patterns that the use of the centrifugal pump is less than ideal, since pulsations in the flow could be observed at the pump frequency. When highly restricted flows were studied such as those through the section pictured in Figure 6 (a) , these pulsations were seen only faintly. In the case of Figure 6 (c), however, the pulsations were quite apparent. The turbine flow meter had no appreciable effect. It was located downstream of the visualization section to minimize its effect on the observed flow.

6.2 Design of Flow Channels

Figure 6 shows the dimensions of the flow channels which were used in acquiring the pictures for this report. In Figures 6 (a) and 6 (b) a closely spaced array of small horizontal perforations in a vertical piece of plastic terminated the flow sections so that the flow appeared infinitely horizontal in direction to upstream fluid elements. In Figure 6 (b) there is a similar upstream device to smooth the velocity profile. Figure 6 (a), however, shows a converging upstream section to assure laminar flow in the channel.

The upper surface of the channel pictured in 6 (a) was roughened to cause "tripping" of fluid elements and subsequent formation of vortices in the boundary layer. The lower surface was milled smooth. This permitted the formation and

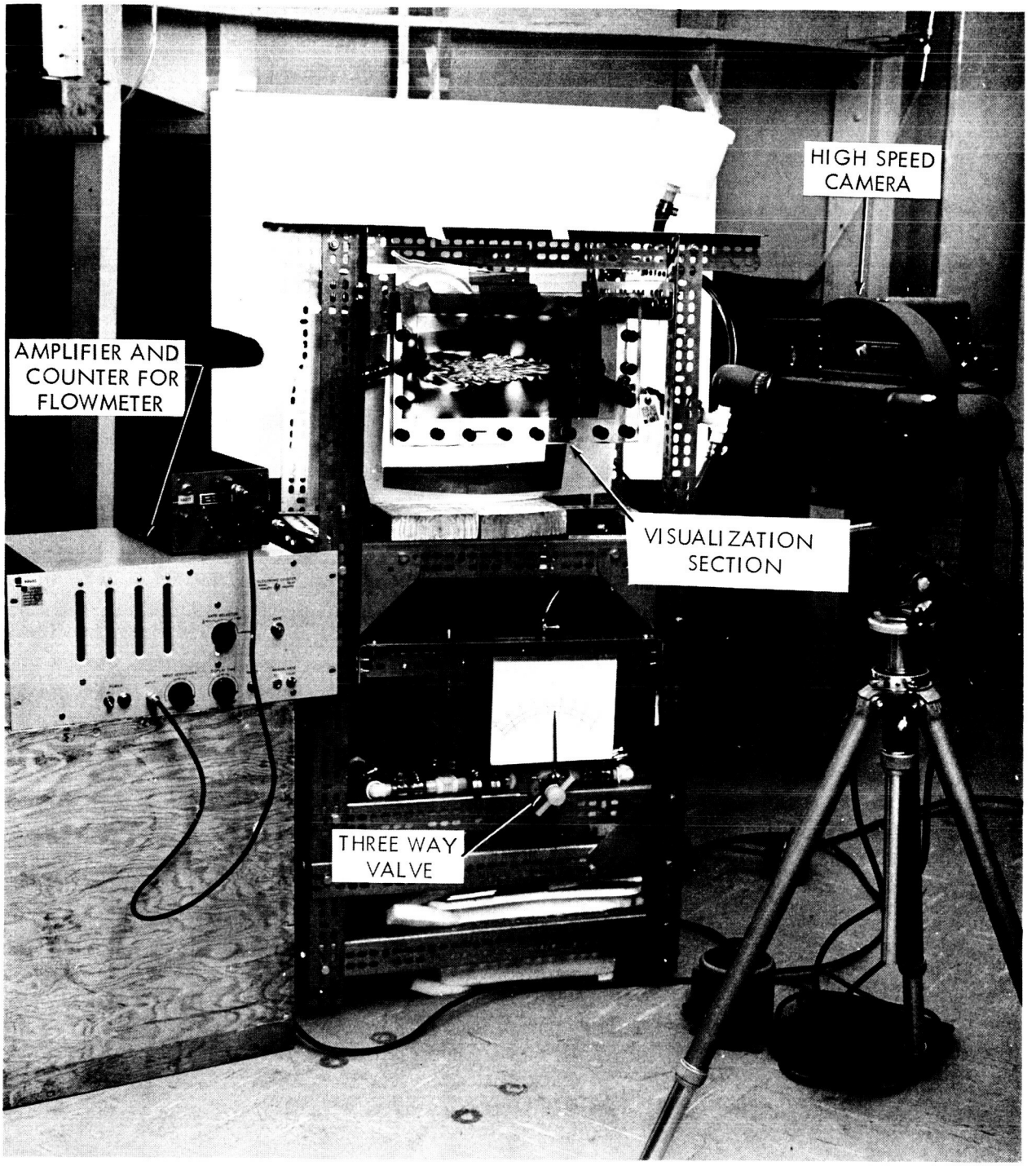

Figure 4. Apparatus Configuration for High Speed Photography.

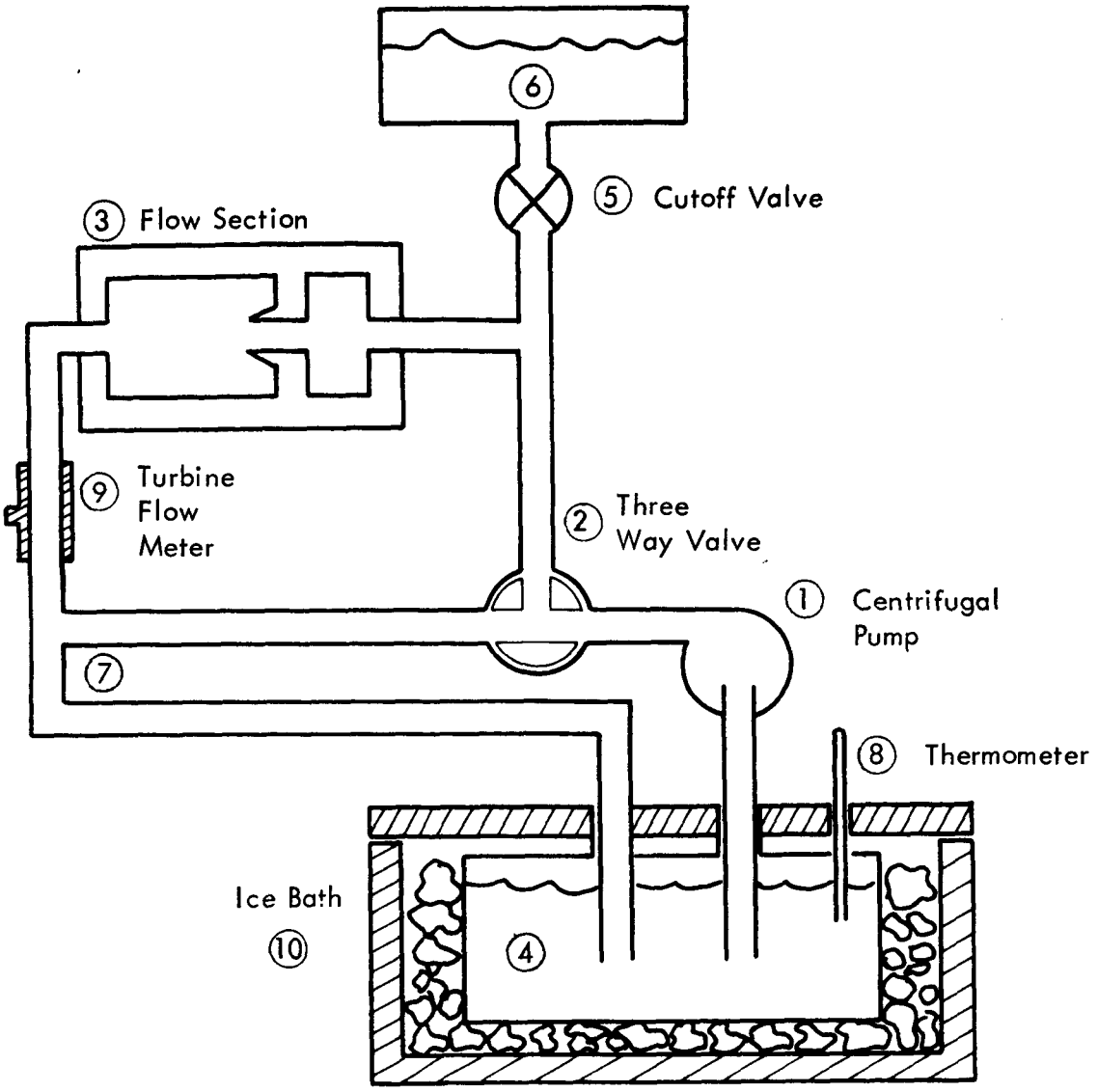

① Gould Chemical Circulating and Transfer Pump Model 4QH, 3450 RPM, 1/8 HP (Stainless Steel)

② Three Way Nylon Valve with 3/4 in. M.I.P.T. Fittings

③ See Figure 6 for Dimensions

④ Polyethylene Reservoir

⑤ Stainless Steel Needle Valve

⑥ Polyethylene Reservoir

⑦ Plastic Hose, 5/8 in. I.D., 7/8 in. O.D.

⑧ Thermometer

⑨ Turbine Flow Meter

⑩ Ice Bath

Figure 5. Physical System Used in Birefringent Flow Visualization

Fluid Thickness 0.125 in.

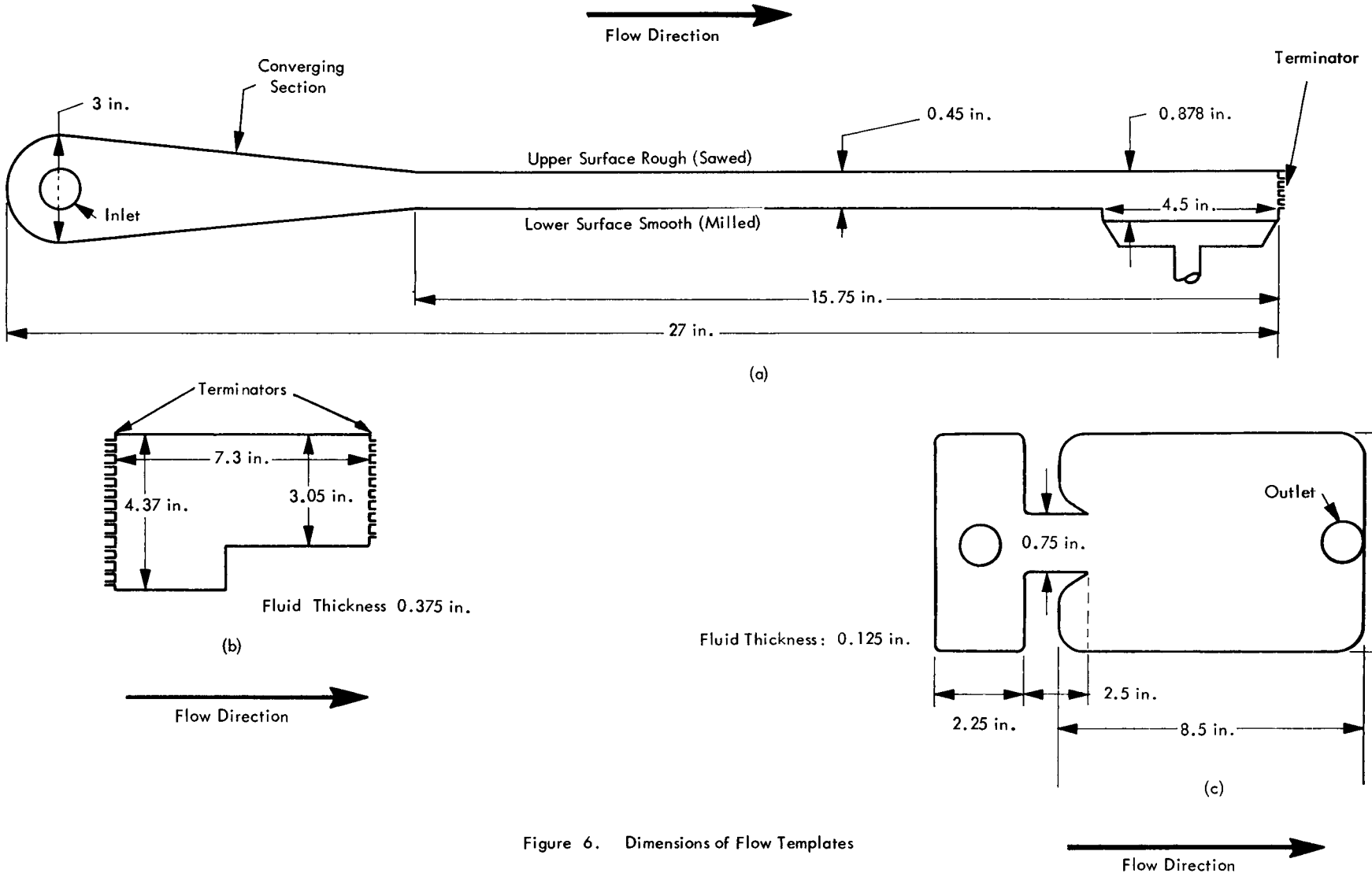

Figure 6. Dimensions of Flow Templates

development of eddy structure adjacent to a single channel surface to be studied. The effect of a discontinuous change in the width of the flow channel on the convected eddies was also observed.

An unfortunate restriction is placed on the design of flow channels if high speed photography is used to document some of the flow features. This means that the channels must be thin so that excessive heating of the fluid by the photographic light will not occur. The relative thinness of the sections is also dictated by the fact that a high light intensity is necessary for photography at a frame rate of about 1700 frames per second. As previously mentioned, a loss of color detail results with increasing optical path length for birefringent materials. This latter effect must also be considered.

6.3 Photographic Equipment and Techniques

Stroboscopic illumination was found to be most useful in studying unsteady or turbulent flows. The decision was therefore made to take high speed motion pictures of some of the more interesting flow phenomena in order that this stroboscopic effect could be documented. Unfortunately, these motion pictures cannot be incorporated into this report, but the general features which may be observed in these films will be discussed in a later section. A "Fastax" camera using "Kodak" Ektachrome EF, Type 7242 film was used in making the motion pictures. An average frame rate of around 1700 frames per second was used. The physical arrangement between subject and camera may be seen in Figure 4.

Color "Polaroid" photographs were also taken of many of the flow patterns. Flash duration was on the order of $5\,(10^{-4})$ second for all still photographs. Many photographs using Type 55 P/N black and white "Polaroid" film packets were also taken. This film provides a positive as well as a negative and is very useful for determining the quality of a picture immediately after the photograph is taken.

Most brilliant colors were obtained with the transmission axes of the polarizer and analyzer at 90° to each other so that the fluid appeared dark when there was no flow. Occasionally however, better detail could be obtained in black and white photographs with the transmission axes parallel. This was especially true in highly turbulent flows.

Various color filters have been tried with the still photographs. Better contrast seemed to be possible in black and white photos using a blue filter. However, improvement in quality, using filters for other colors, was not observed.

7.0 THE LARGE FEATURES OF SEPARATED FLOW, AS VISUALIZED USING FLOW BIREFRINGENCE

7.1 The Role of the Large Eddy in Turbulent Shear Flow

The development of models for large scale eddies,which are consistent with the physical phenomena that are observed in turbulent shear flows,has been of interest to a large number of investigators throughout the field of fluid dynamics. This interest is understandable, since a precise analytical definition of the motions of the largest eddies in a turbulent shear region would be of considerable value in explaining the mean flow properties observed within the region. The manner in which the smaller eddies (that contain and dissipate the greater part of the turbulent energy) are convected, is also clarified by knowledge of the motion of the large eddies.

The mathematical treatment of turbulent shear flows becomes considerably less difficult if a basic unit of the flow structure such as a large eddy has been defined analytically. This unit may then be incorporated either individually or statistically into mathematical models which describe turbulent shear flows.

Townsend (Reference 19) was one of the first to propose a model for the large scale structure in turbulent shear flow. Townsend proposed that a fully turbulent fluid is bounded by convoluted surfaces not unlike those which appear in Figure 11b or 11c. These surfaces are moved about by the convective motion of large eddies which have dimensions of a flow region, throughout which the shear is of the same sign. These eddies are supposed, by Townsend, to be "an order of magnitude" larger than those containing most of the turbulent energy.

Shortly after this, Grant (Reference 20) published data and made conjectures about the large scale eddy structure in a turbulent cylindrical wake.

Lumley (Reference 21) has recently proposed a method for predicting the form of large eddies using empirical data. This technique has been applied with apparent success (to the measurements of Grant) by Payne (Reference 22), using numerical methods. Lumley's method yielded results qualitatively similar to the cylindrical "eddy pair" and "re-entrant jet" model which was proposed by Grant.

A cylindrically shaped "eddy pair" in the wake of a cylinder or in the turbulent mixing region of a two-dimensional jet suggests an obvious extension to the case of a three-dimensional jet. Tung and Ting (Reference 23) have recently determined a zero order solution for the motion and decay of this type of three-dimensional eddy structure in an incompressible viscous field. This eddy structure is referred to as a "vortex ring".

Figure 7 presents an illustration of a vortex ring as it could appear in the fully turbulent region of a circular symmetric fluid jet. This model seems to explain, at least qualitatively, some of the mean flow characteristics in a three-dimensional jet. The case of the three-dimensional jet was chosen as a test case since its mean flow properties have been well verified experimentally and because of its practical importance. The "vortex ring" model, however, need not be restricted to jet flow but may be useful in describing the separated flows which are present on any subsonic cylindrical aero- or hydro-dynamic body where the axis of symmetry of the cylinder coincides with the mean flow direction.

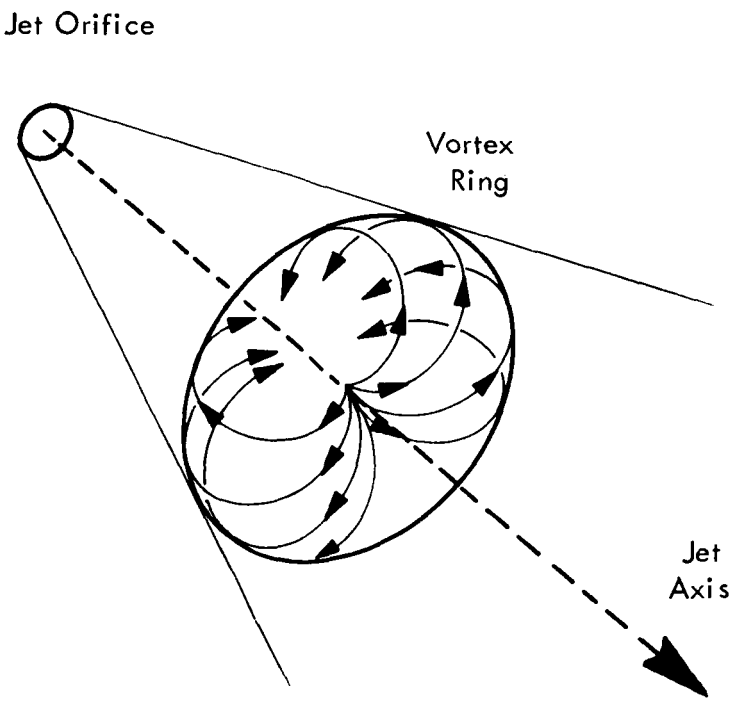

Figure 7. A Vortex Ring in the Fully Developed Turbulent Region of a Circular Jet.

It has been shown in Appendix A that the "vortex ring" model is not inconsistent with the known dependence of axial velocity on distance in a three-dimensional circular jet, using certain physically reasonable assumptions.

A thorough treatment of the "vortex ring" model is beyond the scope of this report, however, and work is still continuing toward establishing the vortex ring as a physically valid and useful model. It is presented in this report as a possible means of

extending the two-dimensional flow patterns, which are observed in the photographs, to the three-dimensional case.

In summary, it may be said that the vortex ring, though almost certainly an over-simplification of the physical case, may be a useful construct for thinking about certain three-dimensional shear flows. The model is not inconsistent with the axial variation of the mean velocity in a three-dimensional jet. Also, the radial variation of angular velocity in a section of such a vortex ring provides an intriguing qualitative explanation of the experimentally observed Gaussian dependence of the mean velocity profile on the transverse jet dimension.

7.2 Channel Flow

Figure 8 shows the flow at three different velocities through a modified form of the channel shown in Figure 6b. The vertical dimension is 3.05 inches along the entire channel length (i.e., there is no step discontinuity as pictured in Figure 6b).

The flow enters the channel through a large array of small fluid jets and exits through a similar jet system. Turbulence is generated by the jet array at the entrance for the two higher flow rates. The decay of turbulence in these two cases is very apparent. It is not difficult to imagine an optical system which would put the observed change in turbulent scale on a quantitative basis by measuring the fluctuations in the intensity of the light transmitted through the flow section.

The boundary layers in the three cases are also visible. In the laminar case the boundary layer is apparently rather broad and the velocity varies slowly in the vertical direction. As the velocity increases, the edge of this boundary region becomes more sinuous and the vertical velocity variation becomes more abrupt. The thickness of the boundary region also seems to decrease as one moves upstream into the region of small scale turbulence. This is consistent with the flattening of the velocity profile which is known to occur in transition from laminar to turbulent flows in pipes and channels.

(a)

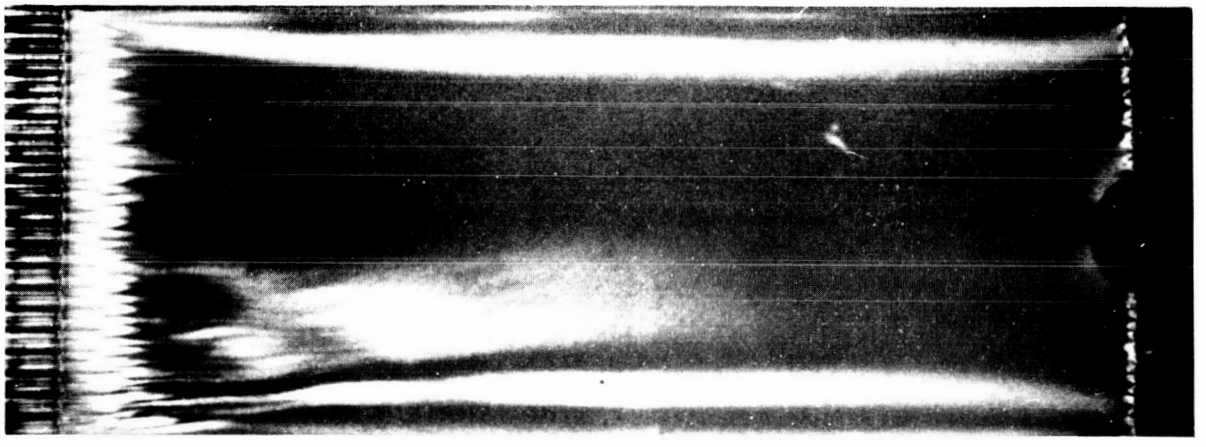

(b)

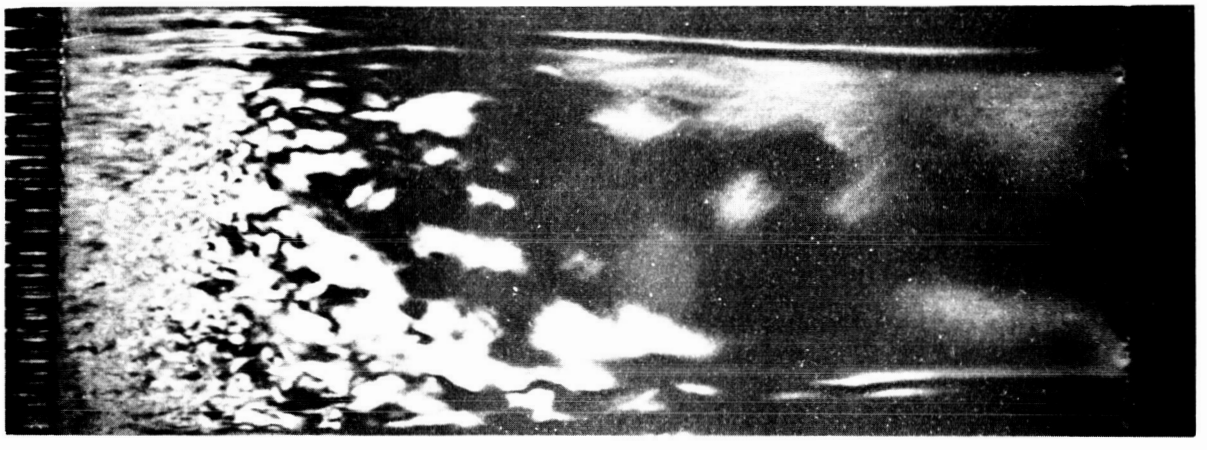

(c)

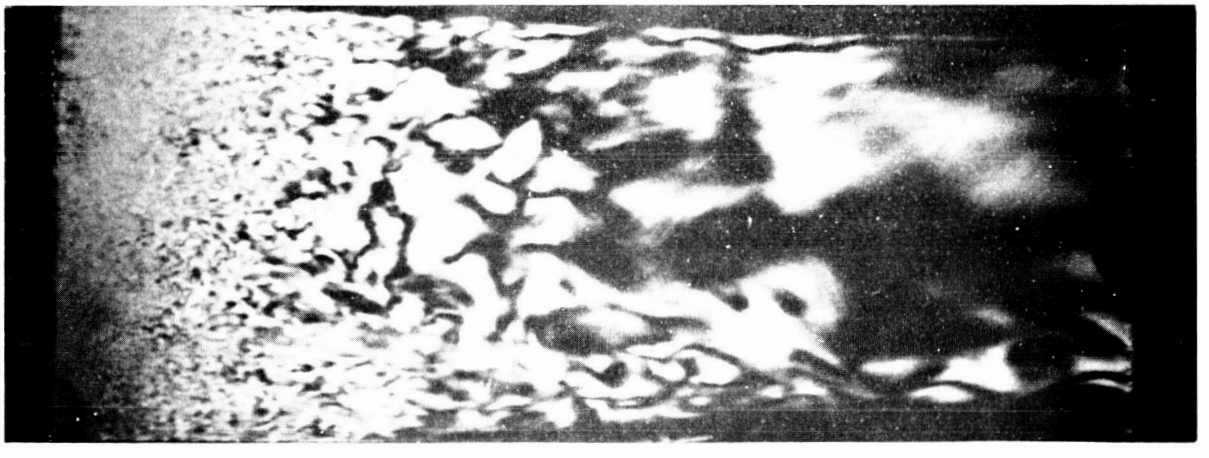

Figure 8. Channel Flow. The velocity is increasing down the page. The flow is from left to right.

7.3 Flow Down a Vertical Discontinuity

Figure 9 is a series of photographs of flow in the channel pictured in Figure 6 (a). An approximate flow velocity for the transition region which is covered by photographs (a) to (c) of Figure 9 is around 12 feet per second. High speed photography was used in studying the flow phenomena in this channel.

The appearance of intermittent bursts of light in the channel recalled descriptions made by other investigators of "turbulent flashes" in pipe or channel flows for the laminar to turbulent transition region. Using high speed photography, the origin of these flashes was determined. The motion pictures clearly show the type of vortex motion shown in Figures 12 (a) and 12 (b). A small vortex is formed by the roughened upper surface of the channel and convected downstream. Such vortices are visible in Figures 9 (c) and 9 (d) upstream of the discontinuity. The upstream vortex system grows slowly in size until reaching the discontinuity. Upon crossing the discontinuity, a von Karman vortex interaction takes place, which is of the type pictured in Figure 12 (b) and photograph (d) of Figure 9. The turbulence downstream of the discontinuity then decays into an eddying structure similar to that pictured downstream of the step discontinuity in Figure 12 (a), and this eddying persists for a prolonged period. The persistence of the eddying motion is probably a result of turbulent mixing in the shear region between the quiescent liquid below the step and the channel flow from upstream. The turbulent mixing flow from a jet should therefore be very similar to flow in this region and similar mathematical analyses or descriptions should apply.

Photograph (e) of Figure 9 shows fully developed turbulence downstream of the discontinuity. Upstream of the discontinuity, a narrow band of laminar flow persists at the smooth lower surface of the channel.

7.4 Flow Up a Vertical Discontinuity

Figure 10 includes three photographs which show flow a different velocities in the flow channel pictured in Figure 6 (b).

Photograph (a) of Figure 10 shows a birefringent pattern which is a result of laminar flow. The boundary layers at all horizontal surfaces are visible and the broad boundary layer originating at the corner of the discontinuity and extending downstream is very apparent. The flow from the upstream array of small fluid jets at the left of the photograph is laminar and only slightly sinuous.

Photograph (b) of Figure 10 is at a slightly higher velocity. The flow from the upstream jet array is now turbulent. The edge of this boundary layer originating at the corner of the discontinuity is slightly sinuous. The other boundary layers begin to show similar trends to those observed in the channel flow shown in Figure 8.

Figure 9. Flow Down a Vertical Discontinuity. The velocity is increasing down the page. The flow is from left to right.

(a)

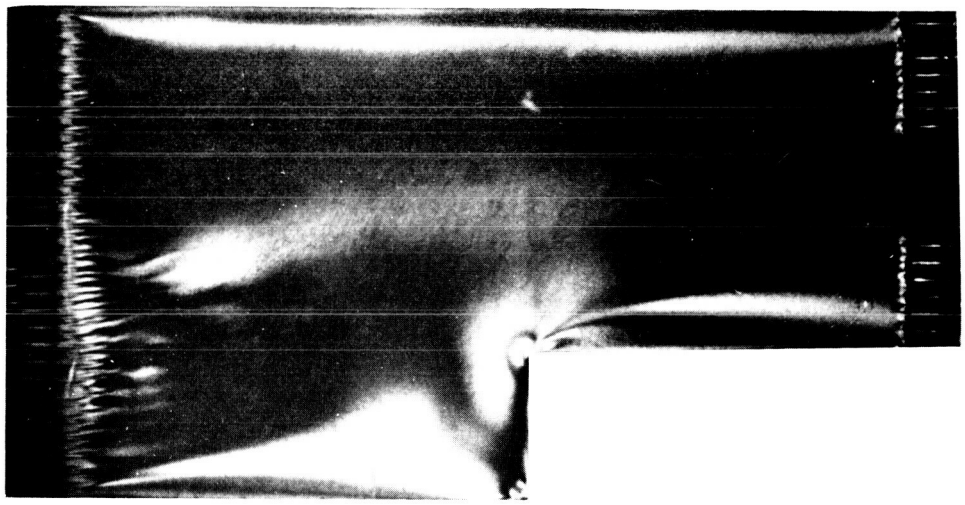

(b)

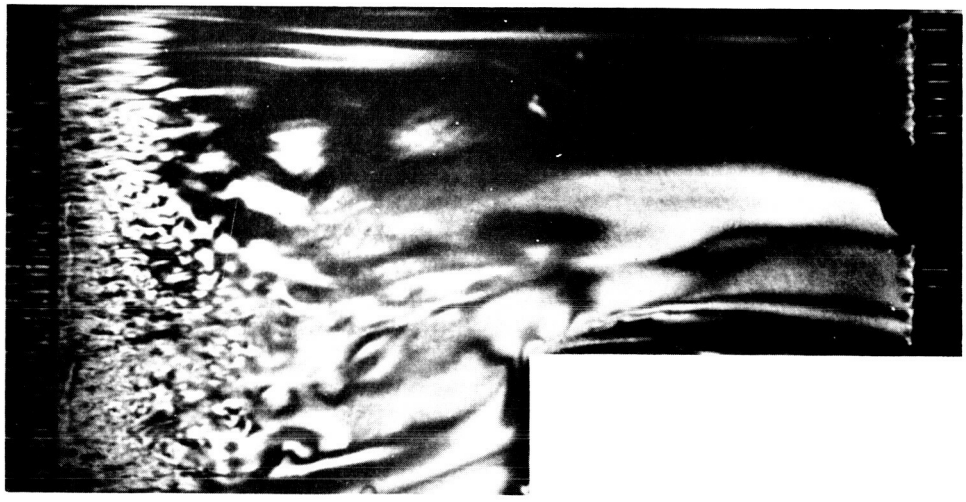

(c)

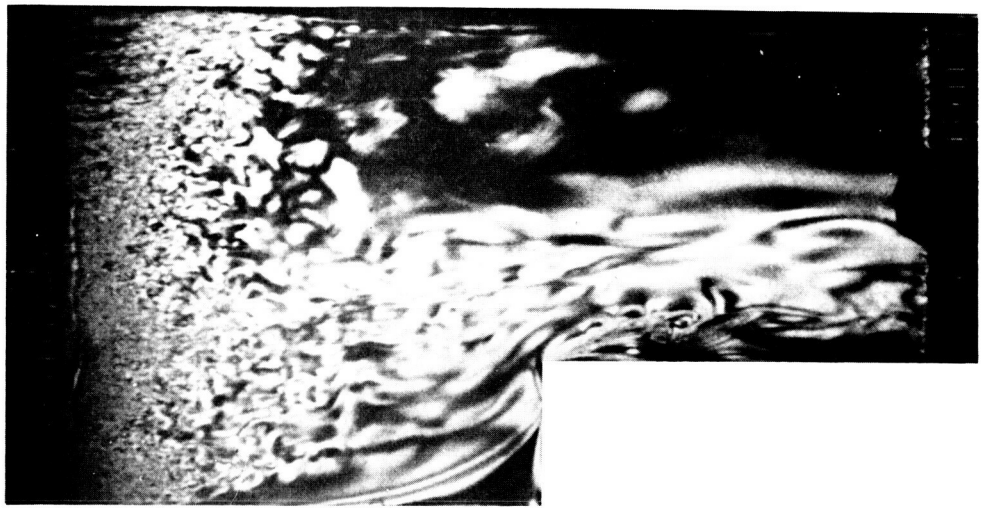

Figure 10. Flow Up a Vertical Discontinuity. The velocity is increasing down the page. The flow is from left to right.

Photograph (c) establishes two trends which cannot occur in the channel flow of Figure 8. The first is the appearance of a clearly visible stagnation region at the foot of the step discontinuity. The second is the formation of a well-defined eddying motion in the boundary layer which originates at the corner of the step discontinuity. The direction of this eddying motion is illustrated in Figure 12 (c). This motion appears to decay a short distance downstream of the discontinuity.

7.5 Jet Flow

Figure 11 and the high speed motion picture associated with this flow configuration (see Figure 6 (c)) for the channel dimensions) are, in many respects, among the most interesting and suggestive photographs obtained in this series.

Unfortunately, regular pulsations (at 60 Hz.) were superimposed on the flow, and the conclusions drawn from these photographs are therefore the most questionable. Pump pulsations in the flow were very apparent under stroboscopic illumination and therefore, the regular pairing of eddies, which is visible in photographs (a) and (b) of Figure 11, may be due to these pulsations.

Figure 12 (d) shows the type of phenomenon observed in the flow. An inner laminar core is visible which has a slightly convoluted boundary surface. The boundary of the jet is also convoluted in a similar manner and the source of these convolutions appears to be large eddy structures of the type proposed by Townsend. It appears that any eddy location on one side of the jet axis may be obtained, approximately, by a reflection about the jet axis of an eddy on the other side. Whether this phenomenon is a result of the pump pulsations, or whether the same symmetry would occur (perhaps, with a random time interval between successive eddy pairs) in the absence of these pulsations, must remain an open question awaiting a more carefully controlled experiment.

As the jet speed increases, the camera became unable to stop as much of the motion. The jet boundaries became less irregular with increasing velocity (see Figure 11) as a result of this. Photograph (c) of Figure 11 shows a fairly linear increase in jet width along the jet axis. This is a well established feature of constant density jets. The lower speed photographs therefore strongly suggest a model for large eddy structure in the mixing region of a constant density jet, although the flow pictured in these photographs is not uniform.

(a)

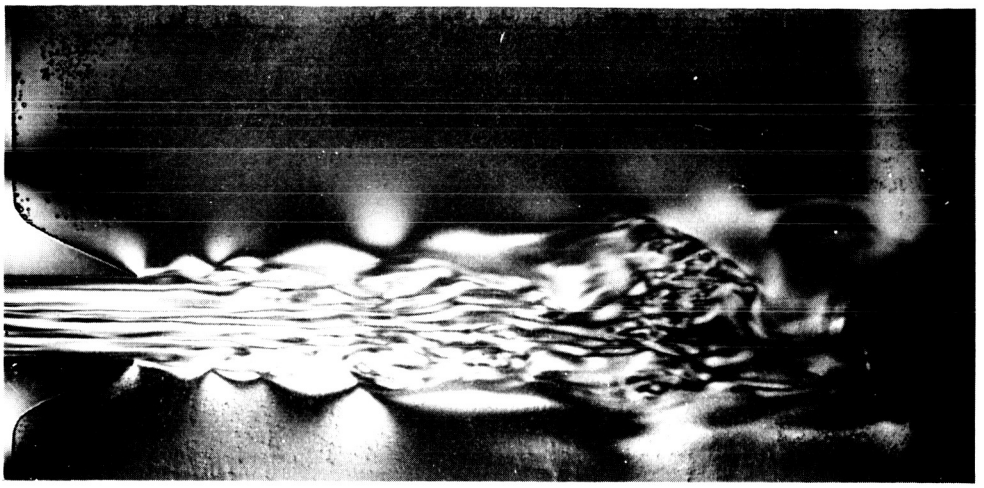

(b)

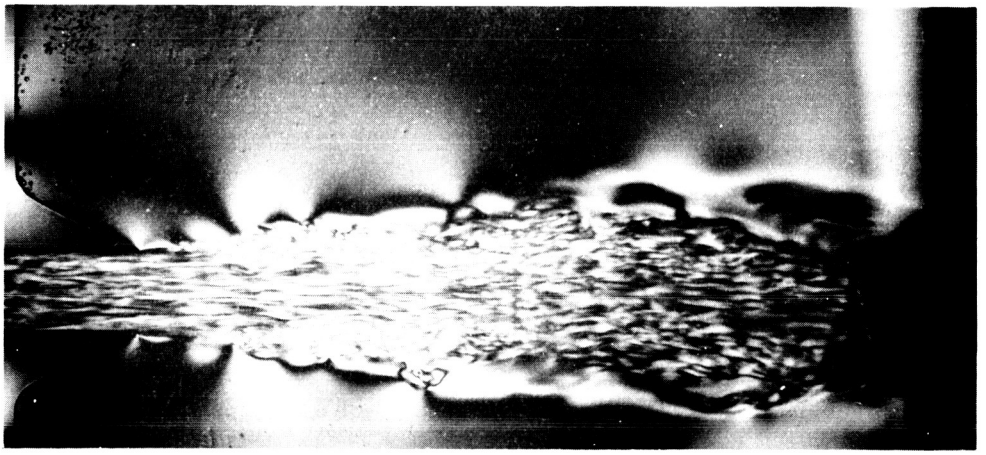

(c)

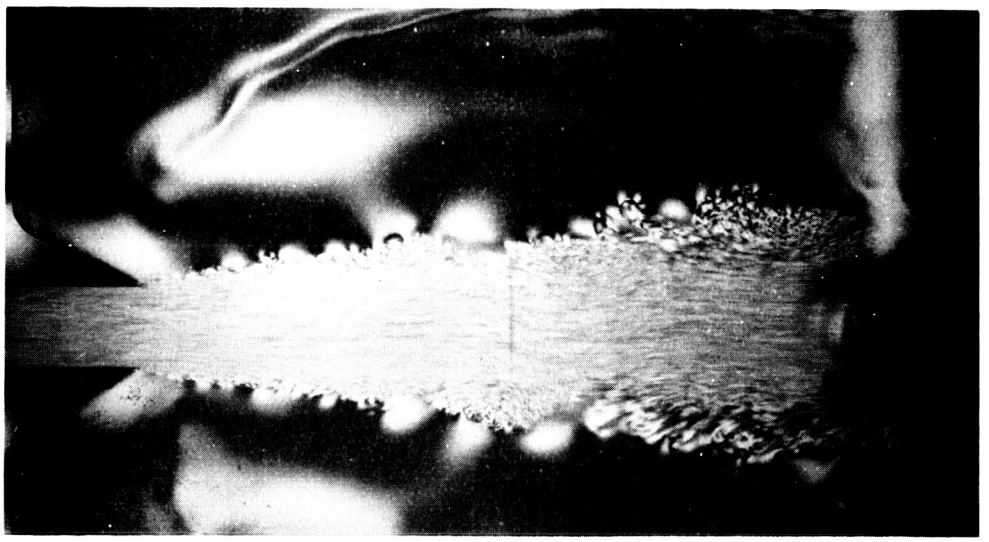

Figure 11. Jet Flow. The velocity is increasing down the page. The flow is from left to right.

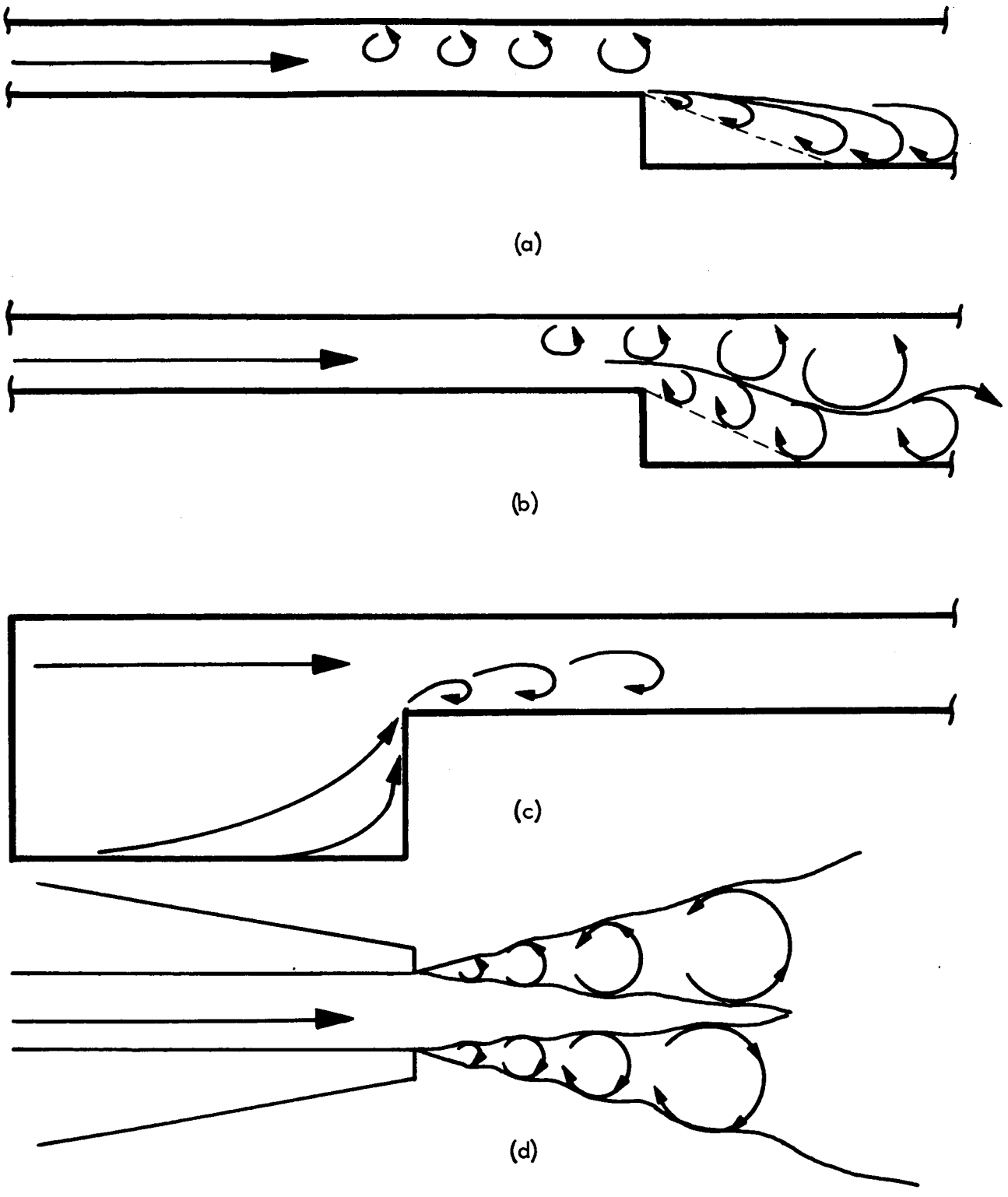

Figure 12. Direction of Rotation of Vortices as Determined by High Speed Photography.

8.0 CONCLUSIONS

Birefringent flow visualization using Milling Yellow Dye Suspension is a valuable tool for qualitative analysis of unsteady flows. This method makes the location of probes in the flow unnecessary. Historically, flow birefringence has been of great value as such a qualitative tool, and has been useful to a number of scientific and engineering disciplines. Also, large eddy structure in turbulent shear flows of MYDS appears to be representative of such flows in Newtonian fluids.

The birefringence of pure liquids shows promise of becoming a useful phenomenon for quantitative analysis of Newtonian flows. Although the birefringence of such fluids is weak, they are more Newtonian in character than strongly birefringent fluids and the theory relating optical and hydrodynamic properties of these fluids is simpler. In order to study unsteady flows by this method, data must be acquired at a point or number of points in the flow field, using an optical system having fast response.

There is loss of color with an increase of optical path length in a birefringent medium. Also, most birefringent liquids absorb light strongly in at least one spectral region. (For instance, MYDS absorbs wavelengths in the blue region.) The use of intense white light is therefore not desirable to visualize thick two or three dimensional flows, unless these strongly absorbed wavelengths are filtered out before the light enters the fluid. This is necessary because heating of the fluid will result in undesirable changes in its optical properties. A better type of lighting would be an intense monochromatic source (perhaps a laser) with a wavelength well removed from spectral regions in which light absorption occurs. A point-by-point quantitative technique using a weakly birefringent fluid might be equally valuable if a relatively small beam of monochromatic light (i.e., a laser) were used. Here again, the light wavelength and the birefringent fluid must be matched to minimize heating of the fluid.

Since the technique of flow birefringence is most definitive when used to visualize two dimensional flows, some method for extending the conclusions drawn from two dimensional geometries to three dimensional cases would be of value. The "vortex ring" model is proposed in this report as one such method of dealing with a large class of turbulent shear flows. The establishment of this model, or any other such simple model which shows a closer agreement to physical reality, could be of considerable value in solutions of certain engineering problems.

Because of the low frequency content of the large turbulent eddies (including those which may possibly be described by the "vortex ring") these models should be of particular value to the studies of low frequency sound generation and flow-induced structural vibration. The relationships between such eddy formations and the mean flow properties should prove especially valuable. These relationships would permit

mean flow properties to be determined from flow visualization experiments. Alternately, they would permit the eddy properties to be inferred from mean flow measurements.

REFERENCES

1. Maxwell, J.C., "On Double Refraction in a Viscous Fluid in Motion," Proc. Roy. Soc. (London), 22, 46-47, (1873).

2. Hauser, E.A., Dewey, "Visual Studies of Flow Patterns," J. Phys. Chem., 46, 212, (1942).

3. Meisner, J.E., Rushmer, R.F., "Eddy Formation and Turbulence in Flowing Liquids," Circulation Research, 12, 455-462, (1963).

4. Leyse, R.M., et al., "Prosthetic Values for Cardiac Surgery," Chapter 3, pp. 56-70; K.A. Merendino, Ed.; Charles C. Thomas, Pub.; Springfield, Ill. (1961).

5. Davila, J.C., et al., "Heart Substitutes," Chapter 3, pp. 37-44; A.N. Brest, Ed; Charles C. Thomas, Pub.; Springfield, Ill. (1966).

6. Attinger, E.O., "Pulsatile Blood Flow," Chapter 9, p. 186; E.O. Attinger, Ed.; McGraw-Hill Book Co., New York, (1964).

7. Baker, W.R., Jr.; Johnston, J.A., Jr., "Optical Differentiation of Amoebic Ectoplasm and Endoplasmic Flow," Science, 156, 825-826, (1967).

8. Rosenberg, R., "The Use of Doubly Refracting Solutions in the Investigation of Fluid Flow Phenomena," David Taylor Model Basin Report 617, AD609632, (1952).

9. Prados, J.W., "The Analysis of Two-Dimensional Laminar Flow Utilizing a Doubly Refracting Liquid," University of Tennessee, Ph. D. Thesis, (1957).

10. Prados, J.W., and Peebles, F.N., "Two-dimensional Laminar-Flow Analysis, Utilizing a Doubly Refracting Liquid," A.I. Ch. E. Journal, 5, 225-234, (1959).

11. Bogue, D.C., Peebles, F.N., "Birefringent Techniques in Two Dimensional Flow," Trans. Soc. Rheology, 6, 317-323, (1962).

12. Peebles, F.N., and Liu, K.C., "Photoviscous Analysis of Two-dimensional Laminar Flow in an Expanding Jet," Experimental Mechanics, pp. 1-6, September (1965).

13. Havewala, J.B., "The Study of the Viscous Properties of Aqueous Milling Yellow Dye Solution at Very Low Shear Rates," University of Tennessee, B.Sc. Thesis, (1958).

14. Peebles, F.N., Prados, J.W., and Honeycutt, E.H., Jr., "Birefringent and Rheologic Properties of Milling Yellow Suspensions," J. Polymer Science: Part C, No. 5, pp. 37-53, (1964).

15. Rossi, B., "Optics," p. 287, Addison-Wesley Publishing Co., Inc., Reading, Mass. (1959).

16. Wayland, H., "Journal of Applied Physics," 26, 1197, (1955).

17. Boeder, P., "Über Strömungsdoppelbrechung," Zeits. f. Physik, 75, 258-281, (1932).

18. Thurston, G.B., Hargrove, L.E., "An Optical Method for Analysis of Fluid Motion," Report No. 1, AD-134151, (1957).

19. Townsend, A.A., "The Structure of Turbulence Shear Flow," The Cambridge University Press, New York, (1956).

20. Grant, H.L., "The Large Eddies of Turbulent Motion," J. Fluid Mech. 3, 149-190, (1958).

21. Lumley, J.L., "The Structure of Inhomogeneous Turbulent Flows," Proceedings of the International Colloquium on Fine-Scale Processes in the Atmosphere and Their Influence on Radio Wave Propagation, Doklady, Akademia, Nauk SSSR, Moscow.

22. Payne, F.R., "Large Eddy Structure of a Turbulent Wake," AD642298, (1966).

23. Tung,C., and Ting, L., "Motion and Decay of a Vortex Ring," Physics of Fluids, 10, 901-910, (1967).

24. Landau, L.D., Lifshitz, E.M., "Fluid Mechanics," pp. 132 and 133, Addison-Wesley Publishing Co., Inc., Reading, Mass. (1959).

25. Corrsin, S., Uberoi, M.S., "Further Experiments on the Flow and Heat Transfer in a Heated Turbulent Air Jet," NACA Report 998, pp. 859-875, (1949).

26. Laurence, J.C., "Intensity, Scale, and Spectra of Turbulence in Mixing Region of Free Subsonic Jet," NACA Report 1292, (1956).

APPENDIX A

THE AXIAL VARIATION OF MEAN VELOCITY IN A CIRCULAR FREE JET

The Coordinate System

The definitions of many of the parameters which are to be used in this discussion may be obtained from Figure 13. A comparison of Figure 13 and Figure 7 may be necessary to visualize the type of system that is under consideration.

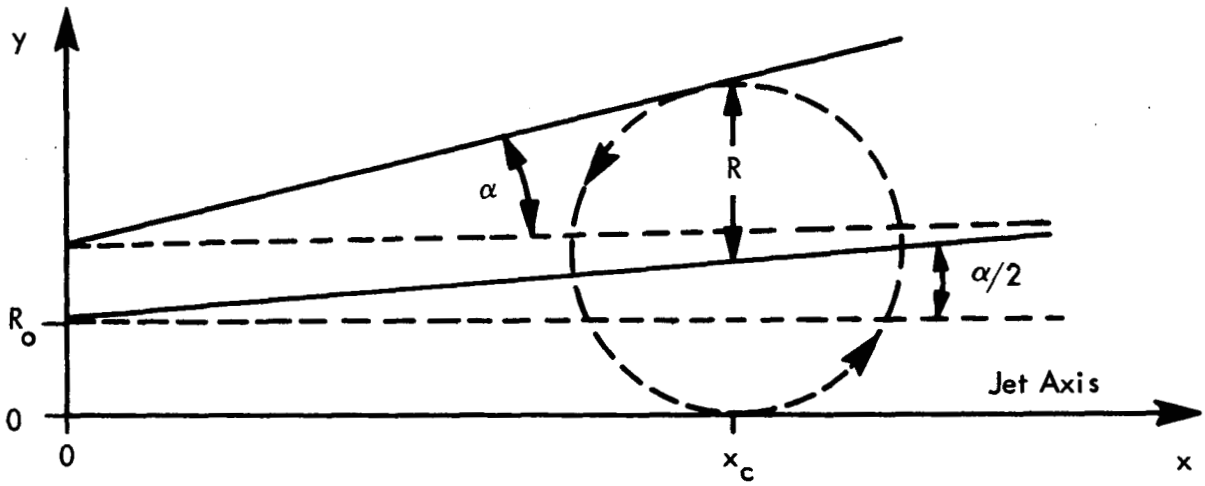

Figure 13. Coordinate System for the Analysis of Vortex Ring Motion. The flow is from left to right.

In order to avoid the complexities involved in a description of the mass entrainment mechanism of large eddies, a simple empirical relationship will be used to relate the radius of a vortex ring to its position on the x axis.

Landau and Lifshitz (Reference 24) give the required relationship. In the notation of this report it is:

$$R = R_o + x_c \tan \frac{\alpha}{2} \qquad \text{(A1)}$$

They give a typical value of $\alpha/2$ lying between 6.25 and 7 degrees. Corrsin and Uberoi (Reference 25) have found that a jet spreads more rapidly if the density of jet is less than that of the receiving medium. They have also predicted this effect using an analytical approach.

Basic Assumptions

1. The radius of the vortex ring is equal in length to one quarter of the transverse jet dimension as proposed by Townsend (Reference 19) and as pictured in

Figure 13.

2. The motion of a vortex ring, after its radius achieves this size, is governed by constants of the motion E_o' and L_o', where E_o' is the total energy of a vortex ring, and L_o' is its angular momentum.

3. E_o' and L_o' are constant throughout the life of the vortex ring. This is consistent with the assumption of Townsend that the large eddies are "an order of magnitude" larger than those which have the largest amount of turbulent energy (and hence dissipate a large proportion of the turbulent energy). Also, by considering the self-preserving inertial properties of the proposed eddy system, one sees that this assumption cannot be too bad.

4. The outermost lamina of the vortex ring is loosely coupled to the ring's internal structure. This assumption seems empirically justifiable if one considers the transverse mean velocity profile and realizes that the fluid in the outermost lamina has the highest velocity and must be largely responsible for mass entrainment.

5. The outermost vortex lamina is all that affects the axial velocity in a circular free jet.

An Elementary Treatment of the Motion of a Vortex Ring Lamina

The constants of the motion for a vortex ring lamina may be expressed as functions of R, if the mass and moment of inertia of the outer vortex lamina are known as functions of, R. These quantities are:

$$M \equiv 4\pi^2 \rho R \int_{R-\delta}^{R} r\,dr = 4\pi^2 \rho \delta^2 R \qquad \text{(A2)}$$

$$I \equiv 4\pi^2 \rho R \int_{R-\delta}^{R} r^3\,dr = 4\pi^2 \rho \delta^4 R \qquad \text{(A3)}$$

where ρ is the density, δ is the lamina thickness, M is the mass and I is the moment of inertia.

The lamina thickness, δ, is taken to be a small constant. The physical significance of this is that δ is a coordinate defining the extension in space of a mean-velocity probe in a direction perpendicular to the jet axis. This dimension is of course not dependent on R. We therefore have:

$$\left.\begin{aligned} E_{ROT} &= \frac{kR^4\omega}{2} \\ E_{TRANS} &= \frac{kR^2\dot{R}^2}{2} \\ L &= kR^4\omega \end{aligned}\right\} \text{ where } k \equiv 4\pi\ \rho\delta, \tag{A4}$$

E_{ROT} is the rotational energy of the vortex ring lamina , L is the angular momentum, E_{TRANS} is the translational energy of the lamina in the R direction, $\dot{R}$ designates the time derivatives of R, and ω is the angular velocity.

Since the angular momentum of a vortex ring is assumed constant with respect to variations in R,

$$\omega = \frac{\omega_o R_o^4}{R^4} \tag{A5}$$

Summing the rotational and translational energies of the element and equating them to a constant energy, E_o, produces the equation:

$$R^4\omega^2 + R^2\dot{R}^2 = \frac{2E_o}{k} \tag{A6}$$

which by substitution becomes:

$$\dot{R}^2 = \frac{A}{R^2} - \frac{B}{R^6} \tag{A7}$$

where $A \equiv \frac{2E_o}{k}$ and $B \equiv \omega_o^2 R_o^8$

The solution for differential equation, A7, is:

$$R = \left\{\left[2A^{\frac{1}{2}}\ t + \left(R_o^4 - \frac{B}{A}\right)^{\frac{1}{2}}\right] + \frac{B}{A}\right\}^{\frac{1}{4}} \tag{A8}$$

which gives the time history of a vortex ring element if we know the parameter $\alpha/2$ (Equation A1) and the above assumptions are valid.

The Average Effect of Vortex Rings on the Mean Axial Velocity in a Free Jet

In view of the rather casual treatment being given this subject, it will not be inconsistent to say that the measuring system which is being considered has a long response time compared to the typical time interval between the passage of two vortex rings. This simplifies the averaging process and the axial velocity, v, can be defined by the expression:

$$v = \omega R + \dot{R}(\tan \frac{\alpha}{2})^{-1} \tag{A9}$$

Substitution into Equation (A9) gives:

$$v = \frac{\omega_o R_o^4}{R^3} + \frac{B^{\frac{1}{2}}}{R}\left[\frac{A}{B} - \frac{1}{R^4}\right]^{\frac{1}{2}} (\tan \frac{\alpha}{2})^{-1} \tag{A10}$$

In terms of the constants of the motion,

$$v = v_r\left(\frac{R_o^3}{R^3}\right) + v_r\left(\frac{R_o}{R}\right)\left[\frac{E_o}{(E_{ROT})_o} - \frac{R_o^4}{R^4}\right]^{\frac{1}{2}} (\tan \frac{\alpha}{2})^{-1} \tag{A11}$$

where $v_r = \omega_o R_o$ and $(E_{ROT})_o = \frac{k R_o^4 \omega_o^2}{2}$

The nondimensional form of this equation is

$$\frac{v}{v_p} = \frac{v_r}{v_p}\left\{\left(\frac{R_o^3}{R^3}\right) + \frac{R_o}{R}\left[\frac{E_o}{(E_{ROT})_o} - \frac{R_o^4}{R^4}\right]^{\frac{1}{2}} \left(\tan \frac{\alpha}{2}\right)^{-1}\right\}, \tag{A12}$$

where v_p is the velocity in the lamina core of the jet. There are two constants in this equation which must be determined by fitting the equation to experimental data. These constants will allow one to draw conclusions about the energies and velocities of an average eddy.

An attempt was made to estimate the magnitudes of v_r/v_p and $E_o/(E_{ROT})_o$. Equation A12 provided the best fit to the higher velocity data of Laurence (Reference 26) which is shown in Figure 14. Choosing a value of $E_o/(E_{ROT})_o$ of 1.50, it was found that a value for v_r/v_p of 0.0865 gave reasonable results, failing only at about 2 diameters from the end of the potential core. The length of the potential core was taken to be 5 diameters and R_o was assumed to approximately

equal D in this rough calculation. A more detailed curve fit of this equation is necessary.

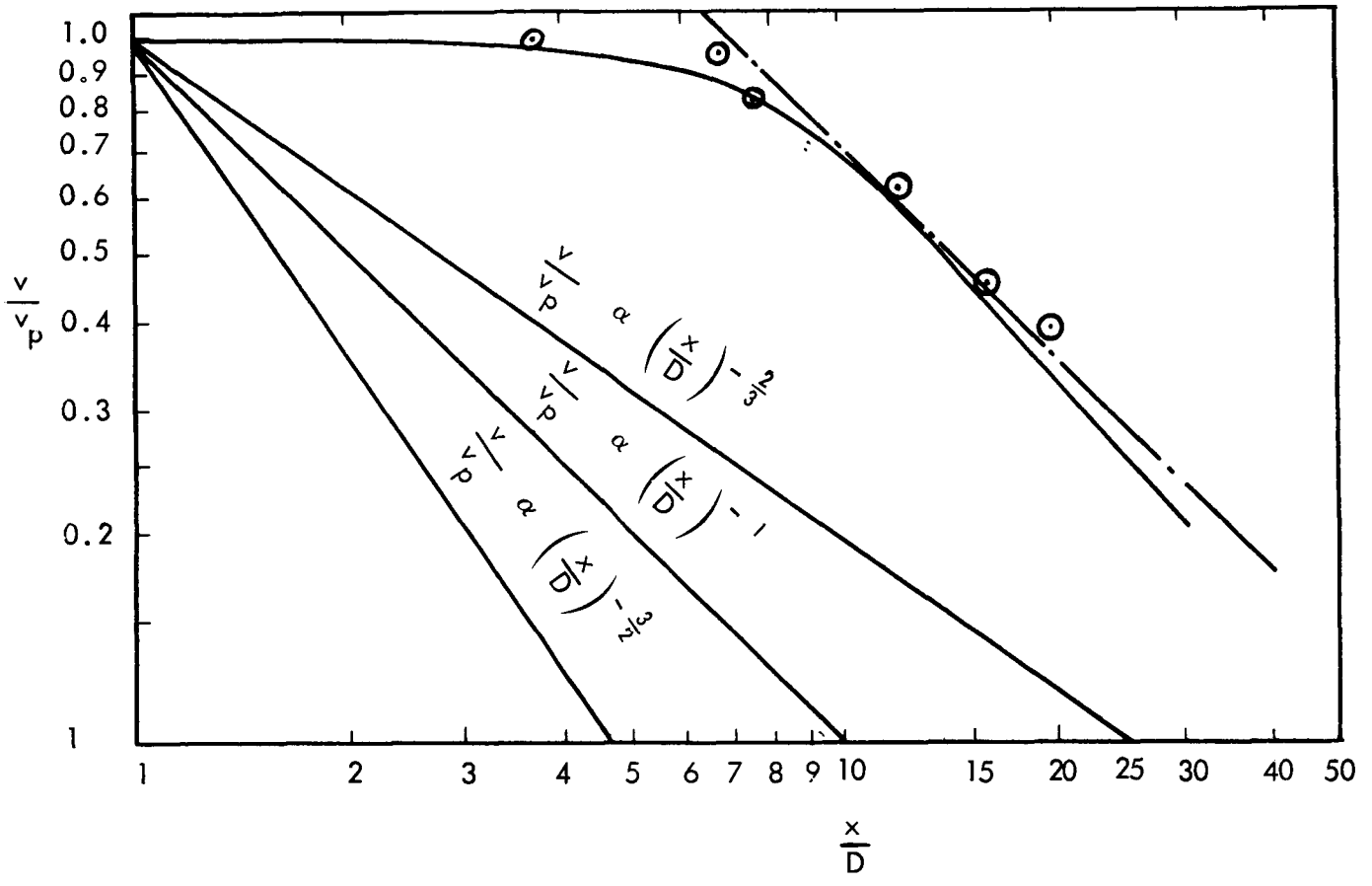

Figure 14. Axial Velocity Variation for a Circular Free Jet.

The solid curved line is data from Reference 25, the data points are from Reference 26. The broken line indicates the relationship

$$\frac{v}{v_p} \propto \left(\frac{x}{D}\right)^{-1} .$$

Figure 14 shows data on circular subsonic jets obtained by two different groups. The data of Laurence (Reference 26) was obtained at Mach numbers ranging from 0.2 to 0.7 while the work of Corrsin and Uberoi (Reference 25) was done at a velocity under 100 feet per second. The data is not inconsistent with the result predicted using the proposed assumptions.